Microscopy and spectroscopy on model catalysts in gas environments

Wenzel, S.

Cover Page

Universiteit Leiden

The handle https://hdl.handle.net/1887/3210401 holds various files of this Leiden University dissertation.

Author: Wenzel, S.
Title: Microscopy and spectroscopy on model catalysts in gas environments
Issue Date: 2021-09-16

Chapter 2
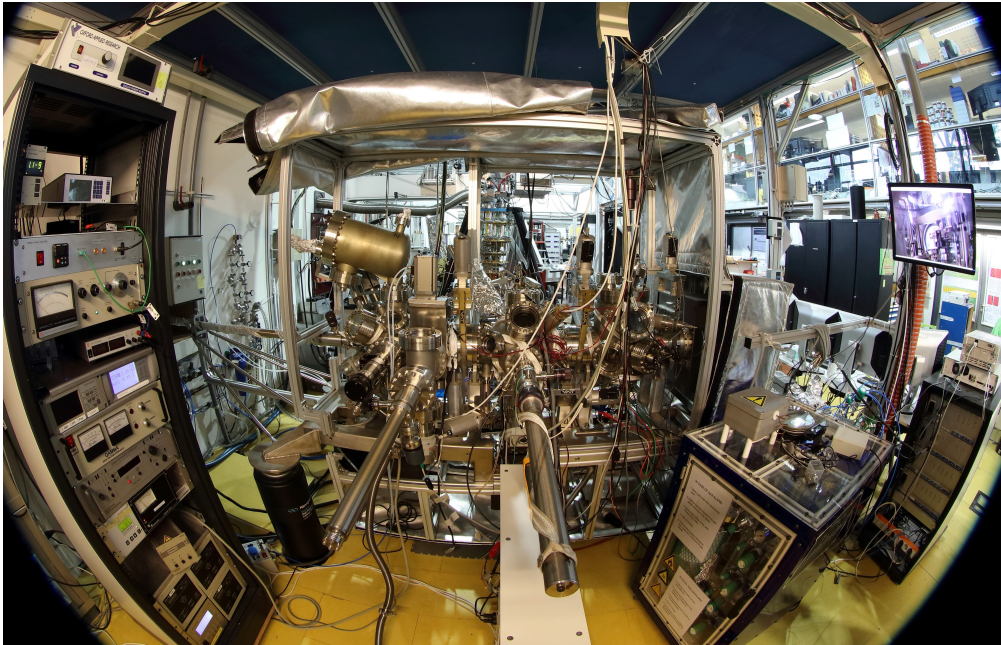
Experimental Techniques

Figure 2.1: Photo of the ReactorSTM setup showing (from left to right) various electronics, the vacuum chamber including the X-ray photoelectron spectroscopy part, the preparation part, and the scanning tunneling microscopy part, the gas delivery system for the flow reactor cell, and the control electronics for the microscope. Photo credit Klaus Wenzel.

2.1   Setups

2.1.1   The ReactorSTM

The measurements presented in Chapters 3 and 4 were conducted on the so-called ReactorSTM at Leiden University, The Netherlands, which is shown in Figure 2.1. This setup is an ultra-high vacuum chamber, in which single-crystal-based samples are prepared and investigated. Hereby, the main component is a scanning tunneling microscope within a flow reactor cell, such that it can image surfaces at ultra-high vacuum pressures as well as in up to 6 bar of gases. This is complemented by vacuum techniques within the same setup: low-energy electron diffraction (LEED), and Auger electron spectroscopy (AES) as well as X-ray photoelectron spectroscopy (XPS). This chapter provides theoretical and technical background necessary for the techniques used.
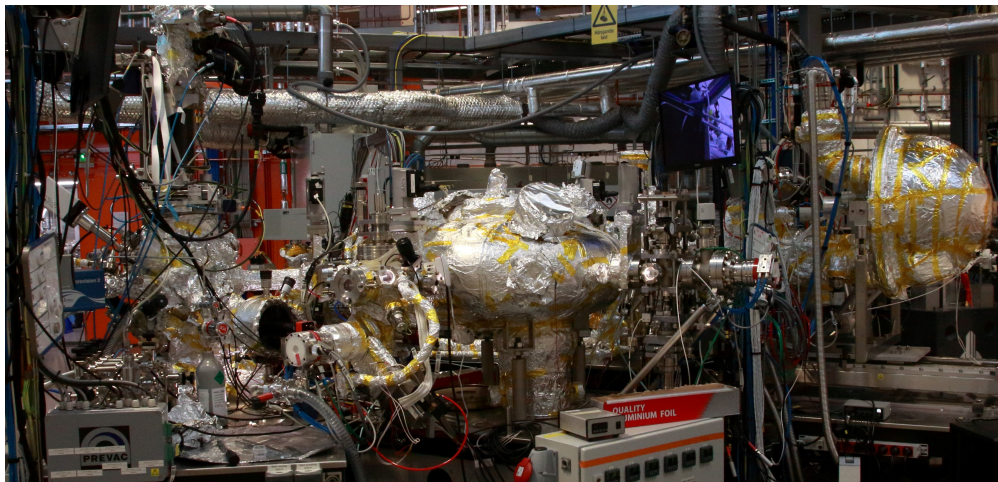
Figure 2.2: Photo of the NAP-XPS endstation of the HIPPIE beamline at MaxIV showing the preparation chamber on the left, a transport chamber in the middle, and the electron analyzer for X-ray photoelectron spectroscopy on the right.

2.1.2 Synchrotron NAP-XPS

The measurements presented in Chapter 5 were mainly conducted at the HIPPIE beamline of MaxIV, Lund, Sweden (see Figure 2.2) and some were conducted at beamline 9.3.2 of the Advanced Light Source, Berkeley, USA. In both cases the endstation consists of a vacuum chamber for sample preparation and synchrotron X-ray photoelectron spectroscopy can be conducted in vacuum as well as in the mbar range of gases. This technique is explained in Section 2.4.

2.2 Ultra-high Vacuum and Gas Handling

Vacuum as well as the use of gas require specialized techniques for creating, maintaining, and monitoring a vacuum, measuring pressures in all ranges, and creating flows of gas. Information on the basic techniques described in this section can be found in fundamental surface-science literature [20,59] and vacuum technology books [60], as well as on manufacturer websites.

2.2.1 Materials

In order to reach ultra-high vacuum the materials inside the chamber cannot have a high vapor pressure, be porous, or contaminated with organic molecules. Additionally, all materials need to be temperature resistant to at least 150 °C as the whole chamber

is heated in order to reduce the water background (see following section). Parts which are close to a sample at elevated temperatures might have to be made of materials resistant to significantly higher temperatures. The main chamber is usually constructed of stainless steel and copper seals for connecting different parts. Filaments and other high-temperature parts can for example be made from tungsten, molybdenum, or tantalum. Ceramics as alumina or sapphire are used for electrically isolating parts.

Parts that come in contact with gases, such as gas lines, valves, and reactor parts can be made from stainless steel for a number of standard gases. However, if gases are corrosive, specialized materials such as gold-coated steel or Hastelloy C have to be used. Additionally, the construction materials should be inert for the reactions to be studied.

2.2.2   Vacuum Pumps

Depending on the pressure range, different types of pumps are used. So-called rough pumps like rotary vane pumps, dry scroll pumps, or membrane pumps can reach a rough vacuum down to a range of 10^{-3} mbar. These are used as pre-pumps for high-vacuum pumps as well as for pumping gases when emptying a reactor or using a reactor through which the gas is constantly flowing.

Turbo molecular pumps, which produce a pressure gradient by rotating blades, can reach the ultra-high vacuum range of down to 10^{-10} mbar and require a rough pump downstream. For applications that require low mechanical noise so-called ionization pumps are useful as they do not have any moving parts or exhaust connections. Ionization pumps ionize and trap the molecules and atoms they pump and can only be used once the 10^{-7} mbar range has been reached with a turbo molecular pump. Independent of the pump that is used, vacuum chambers can only reach ultra-high vacuum in a reasonable time frame when they are heated to at least 100 °C after evacuating the air. During this so-called baking, water adsorbed on the inside of the chamber can desorb and be pumped.

2.2.3   Pressure Gauges

Vacuum pressures in the range from 10^{-4} to 10^{-11} mbar can be measured by ionization gauges. In general these create free electrons which ionize the gas molecules. These are in turn collected creating a current that is a measure for the pressure. If the free electrons are produced using a hot filament (hot filament or Bayard-Alpert gauge) this can cause for example oxygen dissociation as well as the deposition of contaminants from the filament material onto samples. Therefore, so-called cold cathode or Penning gauges can be a more suitable choice. Here the free electrons are produced in a self-supporting discharge which starts from a cathode at room temperature and is

sustained by secondary free electrons created when the ionized gas molecules impinge on the cathode.

Rough vacuum is mostly monitored with so-called Pirani gauges, which make use of the fact that the electrical resistance of a filament is dependent on the amount of heat loss to the surrounding gas environment.

Whereas all pressure gauges described so far measure gas-type dependently, mechanical pressure gauges can measure the pressure independent of the type of gas and directly as force per area. An example is the baratron gauge, which can be used in the intermediate range from 10^{-4} mbar to atmospheric pressures. Here the pressure-dependent position of a membrane is measured as a change in capacitance. Standard mechanical manometers measure pressure with respect to the surrounding atmosphere by detecting the movement or deformation of a solid piece or liquid and displaying it in an analog way. These are used at atmospheric pressures and above like in gas supply lines and bottles.

Precise digital read-out of pressures over a large range can be achieved using piezoresistive pressure sensors, in which the pressure-dependent deformation of a piezoresistive material is measured as a change in its electrical resistance. These are combined with an automatic valve and feedback system in so-called back pressure controllers, which can stabilize the pressure in flow reactors to a chosen set-point.

2.2.4   Gas Supplies

For the use of gas at low pressures inside a vacuum chamber so-called leak valves can be used. These separate the chamber from the atmospheric pressure gas line by a soft material seal pressed against a sealing surface. By decreasing the force against the seal the amount of gas that leaks into the chamber can be increased. The desired pressure and the type of gas determine which vacuum pumps can be used on the chamber while filled with gas.

For a controlled supply of larger amounts of gas to reactors so-called mass flow controllers can be used. These determine the flow by measuring the transport of heat by the gas and are thus gas-type dependent. A feedback controls a valve inside the controller to allow for the desired flow.

2.2.5   Gas Analysis

The residual gas in a vacuum chamber can be monitored with a quadrupole mass spectrometer (QMS). Gas molecules are ionized by free electrons and then accelerated by a fixed voltage. This results in an ion velocity dependent on the charge-to-mass ratio. The quadrupole itself consists of four parallel rods. The same oscillating voltage

is applied to opposite rods with different sign for the two pairs of rods. This leads the ions onto an oscillating path and depending on the voltage only one specific charge-to-mass ratio reaches the detector at the end of the rods whereas all other ions hit the center or the outside wall of the quadrupole. By varying the voltage all desired charge-to-mass ratios can be measured.

A QMS can also be used to measure the reaction mixture or products from a reactor if a small amount of the gas is let into a vacuum chamber with a QMS installed. It can only be operated at pressures up to 10^{-6} mbar. However, the background of the vacuum chamber itself can disturb such gas measurements. A more suitable method for directly analyzing a gas mixture is gas chromatography, which will not be explained here.

2.2.6   Sample Preparation

Controlled surface-science studies in ultra-high vacuum are often done on bulk single-crystal samples. A specific surface face can for example be prepared by cleaving the material in a vacuum chamber or by cutting and polishing in air. Subsequent electrochemical etching and/or ion sputtering in ultra-high vacuum removes contaminants from the material. The cleanliness of the surface can be monitored with different methods in UHV. The indicators used in this work, in the order of increasing sensitivity, are sharpness of the low-energy electron diffraction pattern (see Section 2.5), detection of other materials using spectroscopy (see Section 2.4), and the visibility of foreign atoms in scanning tunneling microscopy images (see Section 2.3).

Sputtering and Annealing

The samples used in this thesis are prepared by sputtering and annealing. The sputtering gun produces free electrons in a filament, which are then trapped in a cylindrical grid. When the vacuum chamber is filled with an inert gas such as argon on the order of 10^{-6} mbar, the free electrons ionize argon atoms. The argon ions are in turn accelerated and focused onto the sample by electrostatic lenses. When impinging on the sample, the positively charged argon ions remove the uppermost layers of atoms of the sample material together with contaminants. As this process roughens the surface it has to be annealed to a temperature of about two thirds of the melting temperature, which flattens the surface again. Heating in ultra-high vacuum can easily be achieved radiatively with a filament behind the sample. The heating power can be increased with so-called e-beam heating where free electrons are accelerated from the filament to the sample. This can either be realized by applying a positive voltage to the sample or by applying a negative voltage to the filament while the sample is grounded. From

the 10^{-4} mbar range of gases on, especially in atmospheric and higher pressures, other heating methods have to be applied. Examples are resistive heaters from ceramic materials in direct contact with the sample and heating by exposure to laser light. The temperature of the sample is monitored using so-called thermocouples, two materials whose electrical behavior depends differently on the temperature. When both are in contact with the sample, a voltage difference can be detected at their other end (at room temperature) as a measure for the temperature of the sample. During annealing, contaminants from the bulk of the sample segregate to the surface. With repeated cycles of sputtering and annealing the density of contaminants on the surface and up to a certain depth into the bulk is reduced over time.

Physical Vapor Deposition

Other metals, oxides, and sulfides can be deposited onto a single-crystal substrate via physical vapor deposition using for example a so-called e-beam evaporator. A rod of the desired material is heated using a filament and a positive high voltage on the rod. Once the material starts to sublime, it can be deposited onto the sample in vacuum or gas background.
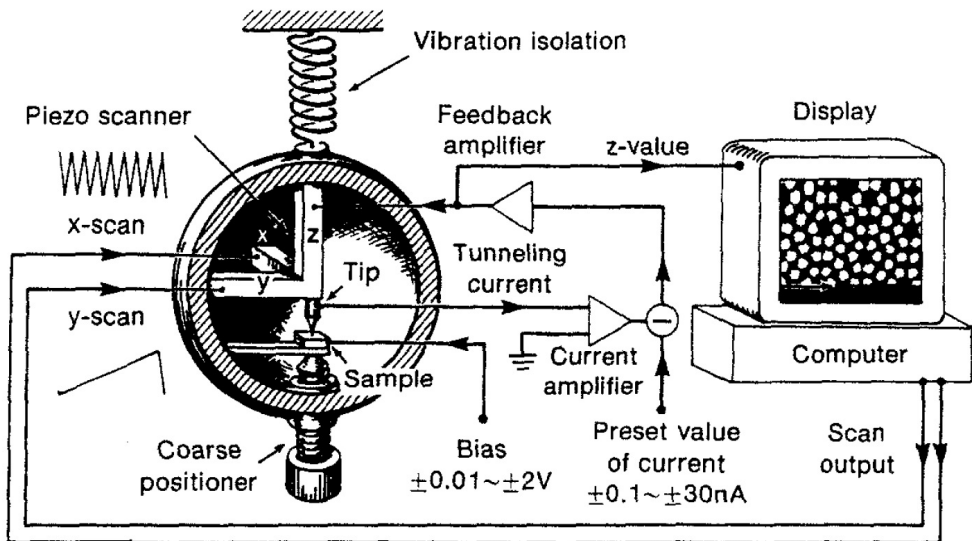

Figure 2.3: Schematic of a typical scanning tunneling microscopy setup. Figure reprinted from Ref. [61].

2.3   Scanning Tunneling Microscopy

Scanning tunneling microscopy, as invented by Binning and Rohrer in 1982 [62,63], allows for atomically resolved imaging of surfaces in vacuum as well as in gases and liquids. The following sections introduce the basic principle and components of a scanning tunneling microscope (STM) based on standard literature [20,61]. Figure 2.3 gives an overview of these components.

2.3.1   General Physical Principle

The scanning tunneling microscope makes use of the principle of electron tunneling. In the quantum mechanical description, the position of an electron is not known exactly but described by a wave function that can be understood as the probability for the electron to be in certain positions. These wave functions partially reach into classically forbidden areas where the potential is higher than the energy of the electron. It follows that there is a non-zero probability for an electron to cross such a potential barrier. This probability decreases exponentially with the width of the potential barrier. This is used in a scanning tunneling microscope where an atomically sharp tip is brought as close to the sample as a few Å. While applying a so-called bias voltage between tip and sample, electrons can tunnel through the vacuum (gas or liquid) in between them, which can be measured as a so-called tunneling current. As this current is dependent on the distance between tip and sample, it can be used as a measure for height changes on the surface while the tip moves across the surface. However, one has to keep in mind that the tunneling current is determined by the local density of electron states and thus not only dependent on the distance between tip and sample but also on the local electronic structure. This can have significant influence on the interpretation of STM data, especially when (partially) isolating compounds are present on the sample surface. When the bias voltage on the sample is negative, the STM image shows the occupied electronic states in the surface (filled-state scanning). A positive bias voltage on the other hand is used to image the unoccupied electronic states (empty-state scanning).

2.3.2   Positioning system

A crucial part of every scanning tunneling microscope is the positioning system as shown in Figure 2.3. First, the tip and sample need to be brought into tunneling distance with a coarse positioning system. Then the tip needs to be able to move in all three directions in small increments on the Å scale. This can be achieved with three independent piezoelectric motors. These are made from materials which expand and contract depending on the voltage that is applied across them. The piezoelectric motors which move parallel to the surface can be used to move to a certain position on
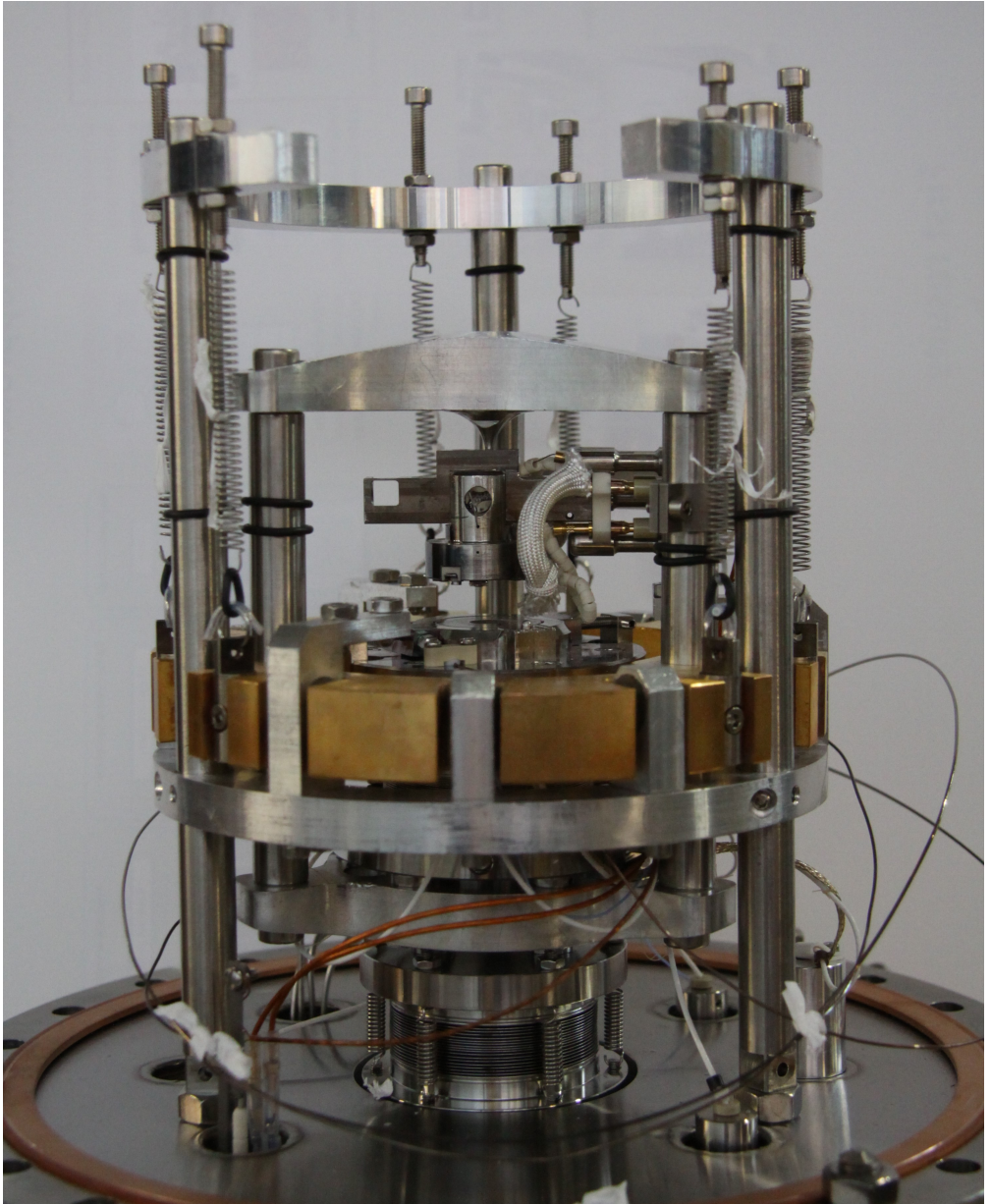
Figure 2.4: Photo of the STM part of the ReactorSTM setup showing the eddy current damping system with the sample holder in the center. The sample (not visible) is facing down.

the surface. During scanning, one direction (x in this thesis) oscillates quickly while the other (y in this thesis) is changed gradually. This constitutes a scanning motion over the surface allowing the recording of two-dimensional images. Finally, the piezo that moves the tip normal to the sample surface (z in this thesis) is needed to move into a suited tunneling distance. In constant-current mode (see Section 2.3.3) the z motor additionally moves while scanning over the surface.

2.3.3   Scanning Modes and Feedback Circuit

On sufficiently flat samples, scanning tunneling microscopes can be used in the constant-height mode. In this case the tip is scanning across the surface at a constant height while the tunneling current is recorded and used as a measure for the corrugation of the surface. While this allows for fast scanning it is not suited for more corrugated surfaces, on which the risk of contact between tip and sample is too high in the constant-height mode. Instead the constant-current mode is used. In this case a feedback circuit is used that moves the z-position of the tip in such a way that the tunneling current stays at a fixed set-point value. The error between the measured tunneling current and the set-point functions as the input for the feedback circuit. The feedback circuit then calculates the necessary change to the z-position as a function of the error itself (proportional) as well as the integrated error over a specific time (integral). Choosing the right parameters for the proportional and integral gain, the response time and accuracy of the feedback circuit are optimized. This is necessary in order to limit the possible scanning speed as little as possible.

2.3.4   Vibration Damping and Electrical Interference

As the positioning of the tip and the distance between tip and sample need to be precise and stable on the Å scale, scanning tunneling microscopes need to be isolated from mechanical movements. In the microscope used in this thesis this is done in multiple stages. First, the floor underneath the setup is disconnected from the floor around it. Second, the setup is mounted on pressurized air legs. And last, the microscope itself is suspended from soft springs within the setup (see Figure 2.4). Fixed magnets next to the suspended part slow down any movements of the copper base of the microscope via eddy current damping. As tunneling currents on the order of pA have to be measured by the STM electronics, they have to be properly shielded from electronic interference as well. A separate physical ground connection is crucial. It can be necessary to decouple the STM electronics from other electronics on the same experimental setup, turn other electronics off, and use differential cables for the tunneling current signal.
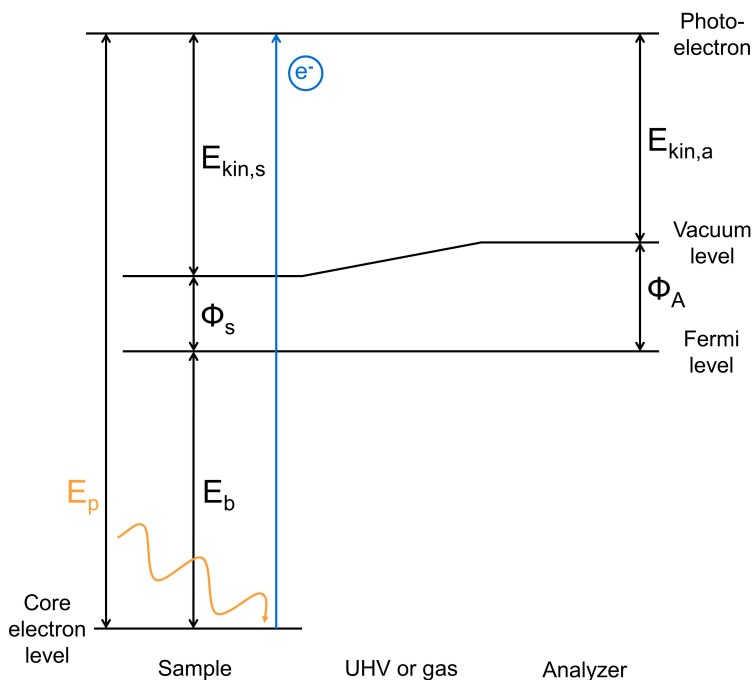
Figure 2.5: Illustration of the energy levels involved in emission and detection of X-ray-induced photoelectrons.

2.3.5 In Situ Scanning Tunneling Microscopy

Scanning tunneling microscopy can in general be used in situ without significant technical effort. However, the gas or liquid does interact with the tunneling electrons as well as the tip and influences the scanning behavior and resolution. The unique feature of the in situ microscope used in this thesis [44], is that the in situ reactor is incorporated into an ultra-high vacuum chamber. This does not only allow for controlled sample preparation in UHV but also for imaging in UHV before and after in situ measurements without exposing the sample to air in between.

2.4 X-ray Photoelectron Spectroscopy

X-ray photoelectron spectroscopy (XPS) identifies the elemental composition of surfaces as well as chemical states. The technique is introduced in general surface-science literature such as Ref. [20] and detailed information can for example be found in Ref. [64]. Originally a UHV technique, XPS is currently also applied in the mbar range of gases and bar range of liquids.
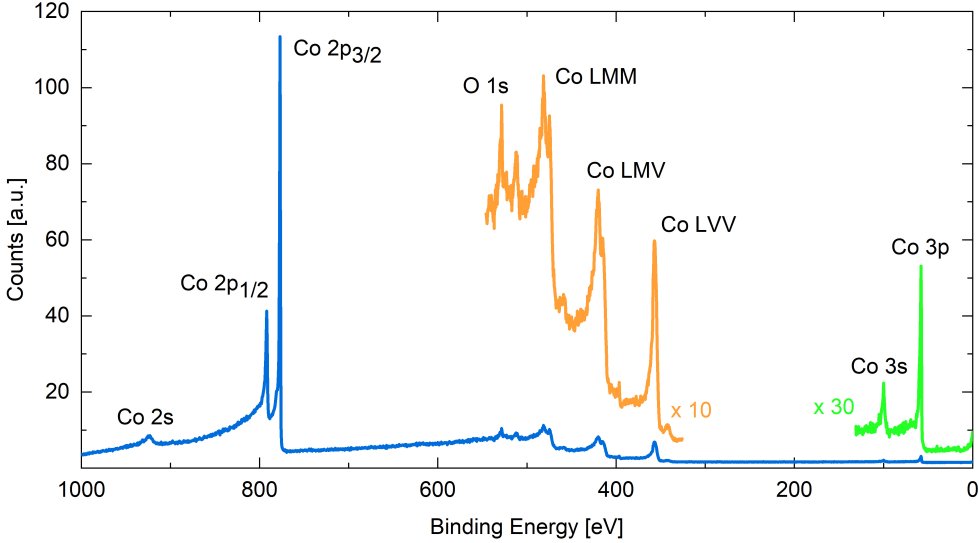
Figure 2.6: Survey X-ray photoelectron spectrum of a Co(0001) surface taken in UHV at 220 °C with a photon energy of 1130 eV. The different peaks are identified using Ref. [65]. Details see text.

2.4.1   General Physical Principle

X-ray photoelectron spectroscopy makes use of the photoelectric effect, which is the ejection of electrons from materials when irradiated with photons. As illustrated in Figure 2.5, the initial energy of the photon E_{p} is hereby split up into the binding energy of the electron in the material E_{b}, the work function of the sample material Φ_{s}, and the remaining kinetic energy of the electron $E_{\mathrm{kin,s}}$ according to $E_{\mathrm{p}} = E_{\mathrm{b}} + \Phi_{\mathrm{s}} + E_{\mathrm{kin,s}}$. Depending on the work function Φ_{a} of the analyzer, the vacuum level close to the analyzer differs from the vacuum level close to the sample by $\Phi_{\mathrm{a}} - \Phi_{\mathrm{s}}$. The analyzer thus measures a kinetic energy $E_{\mathrm{kin,a}} = E_{\mathrm{kin,s}} - (\Phi_{\mathrm{a}} - \Phi_{\mathrm{s}}) = E_{\mathrm{p}} - E_{\mathrm{b}} - \Phi_{\mathrm{a}}$. As the photon energy E_{p} is known, a material with a peak of known binding energy E_{b} or the Fermi edge of a material can be used to determine Φ_{a} and thus calibrate the binding energy axis. In this way the measured kinetic energy spectrum can directly be converted into a measured binding energy spectrum.

2.4.2   Components of XPS Spectra

An X-ray photoelectron spectrum consists of multiple structures. First, the core level peaks of each element which is sufficiently abundant in the sample are visible. The binding energy of a core electron depends on the shell $n = 1, 2, 3, ...$, the angular

momentum $l = 0, 1, 2, 3, ...$, referred to as s, p, d, f, ..., and the total angular momentum (which includes the electron spin) $j = 1/2, 3/2, 5/2, ...$. The energy levels with the same angular momentum l but different spin ($s = + 1/2$ or $- 1/2$) have a fixed occupancy ratio and energy difference. Therefore, the XPS peaks of such a so-called doublet, for example $2p_{3/2}$ and $2p_{1/2}$, have a fixed separation in energy as well as peak-area ratio. An example of such a doublet with an energy spacing of 15 eV can be seen in the survey spectrum of cobalt displayed in Figure 2.6. Apart from the Co 2p doublet the Co 2s, Co 3s, and Co 3p core level peaks are visible. Additionally, some adsorbed oxygen on the cobalt surface causes an O 1s contribution. In general, the exact position of a core level peak depends on the chemical environment the atom is in.

If an X-ray gun without monochromator is used, additional satellite X-ray energies are emitted, which lead to satellite peaks in the XPS spectrum. Similarly, synchrotron X-rays are accompanied by higher harmonics, photon energies which are multiples of the main photon energy, and cause additional (significantly less intense) XPS peaks.

Additionally, the shape of XPS spectra is determined by different loss processes, through which the emitted photoelectrons can lose a part of their energy before leaving the sample material and being detected: First, due to inelastic scattering of photoelectrons the background on the high binding-energy side of a peak is higher than on the low binding-energy side, which can be seen in the survey spectrum in Figure 2.6. This can be taken into account by using the so-called Shirley background subtraction. Second, photoelectrons can also excite so-called bulk as well as surface plasmons, oscillations of the conduction band electrons in metals. This leads to distinct plasmon loss peaks on the order of 10 eV above the main photoelectron peak with possible higher harmonics. Third, the atom can remain in an excited state when the photoelectron is emitted leaving it with a few eV lower energy forming a so-called shake-up peak. Shake-off features appear when the photoelectron loses energy through interaction with valence electrons. In metals with a high electron density close to the Fermi edge such interactions can excite electrons into empty states above the Fermi edge. This causes a tail on the high binding-energy side of the photoelectric peak instead of discrete shake-off losses. The resulting asymmetric peak shape can be described using specific asymmetric line shapes and asymmetry parameters from literature. The Co 2p doublet in Figure 2.6 contains both an asymmetric main peak caused by shake-off losses as well as discrete plasmon losses as can be seen in a detailed fit in Figure 5.1 in Section 5.2.2. Last, if an atom has unpaired electrons in the outer shell, an unpaired core electron produced by photoelectron emission can couple with the unpaired outer shell electron in a number of different ways resulting in different photoelectron energies. These are visible as so-called multiplets in the XPS spectrum.

In XPS spectra (broader) Auger peaks are visible as well. When the core hole left in an energy level n_a after photoelectron emission is filled with an electron from a higher energy level n_b, energy is released. This energy can cause another electron from an energy level n_c to be emitted from the material. This so-called Auger electron causes a peak in the spectrum denoted as $n_a n_b n_c$. Here the nomenclature $n = 1, 2, 3, ...$ is replaced by $n =$ K, L, M, ..., V with V for valence electrons. In the cobalt survey (see Figure 2.6) the Auger peaks Co LMM, LMV and LVV, each consisting of multiple peaks caused by the sublevels in each shell, are visible. The kinetic energy of Auger electrons is element specific and independent of the initial photon energy. Depending on the X-ray source Auger peaks thus appear at different binding energies in the XPS spectrum.

2.4.3 X-ray Sources

In conventional lab X-ray guns, electrons from a filament are accelerated into an anode material. Depending on the material one specific wavelength of photons is emitted. Common are the aluminum K_α line at 1486.6 eV and the magnesium K_α line at 1253.6 eV. Additionally, satellite peaks as well as bremsstrahlung are produced. A monochromator can be used to select only a narrow width from the spectrum around the primary line and thus improve the energy resolution of the instrument.

In synchrotron X-ray sources, photons are emitted from electrons which are kept on a circular path by a magnetic field. Undulators are used to select a specific photon energy. By tuning the photon energy, different probing depths into the material can be achieved. Compared to X-ray guns, synchrotrons produce a significantly larger amount of photons per time and area as described by the so-called brilliance. This allows for a lower detection limit.

2.4.4 Electron Analyzer

The most common type of electron analyzer used in X-ray photoelectron spectroscopy is the concentric hemispherical analyzer. First, an electrostatic lens focuses photoelectrons emitted from the sample into the analyzer. Additionally, it decelerates all electrons by the same amount such that those with the kinetic energy $E_{\mathrm{kin,a}}$ to be detected are left with the so-called pass energy. Second, two concentric hemispheres with voltages V_1 and V_2 act as a hemispherical capacitor and bring the electrons onto a circular path. As the radius of the motion depends on the kinetic energy of the electrons they are separated spatially. The voltage difference $V_2 - V_1$ is chosen such that those electrons with the pass energy hit the detector area and their count is a measure for the amount of photoelectrons with $E_{\mathrm{kin,a}}$. While increasing the deceleration by the

input lens over time, the spectrum is measured from low to high kinetic energy, thus high to low binding energy. The lower the pass energy is chosen, the better the energy resolution of the analyzer. However, a lower pass energy results in a lower overall signal as well.

2.4.5 NAP-XPS

In recent years XPS systems for use in the mbar range of gases have been developed, see for example Ref. [66], which allow for in situ spectroscopy studies of model catalysts. The main challenges are that the electron analyzer can only be operated in vacuum below 10^{-6} mbar as well as the short mean free path of electrons in the gas. Therefore, the most popular design is a differentially pumped system with multiple turbo molecular pumps where the pressure is decreased in stages between the near-ambient pressure region and the electron analyzer. By placing the nozzle between the near-ambient pressure area and the first pumped stage as close as possible to the sample, as many electrons as possible are collected. However, this is limited by the ability of the X-rays to still reach the probed sample area as well as the pressure drop close to the nozzle. Overall, this results in an optimal sample-nozzle distance of roughly 1 to 1.5 times the nozzle diameter. The nozzle diameter can be optimized depending on the requirements for signal strength and gas pressure. In sufficiently large gas pressure, electron attenuation by the gas is pressure dependent and might have to be taken into account during data analysis. Additionally, near-ambient pressure XPS allows for the detection of so-called gas-phase peaks which stem from photoelectrons emitted directly from the gas molecules. As opposed to peaks stemming from the sample, gas-phase peaks shift with the work function Φ_s of the sample. This shift can be used for direct work function measurements [67,68] and thus indicate changes in the overall oxidation state of the sample.

2.5 Low-Energy Electron Diffraction

Low-energy electron diffraction (LEED) is a standard surface-science technique used in ultra-high vacuum in order to determine the structure of crystalline surfaces as well as ordered adsorption structures. Detailed information can be found in general literature such as Ref. [20].

2.5.1 General Physical Principle

The principle of low-energy electron diffraction can conveniently be described in the wave description of quantum mechanics. Electrons with an energy between 30 eV and
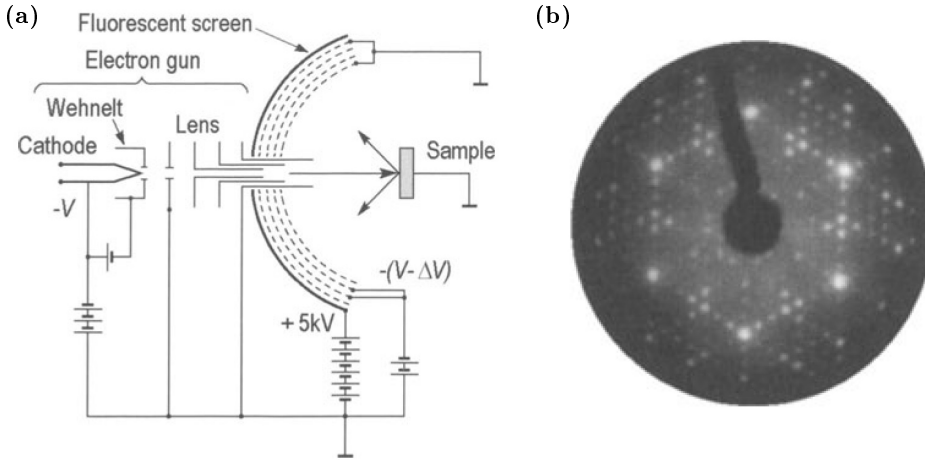
Figure 2.7: (a) Schematic of a LEED setup and (b) typical LEED measurement showing the Si(111) 2x1 reconstruction. Figure reprinted from Ref. [20] and adjusted.

200 eV are waves with a de Broglie wavelength of one to two Å. As this is slightly shorter than the atom-to-atom distance in typical crystalline surfaces, the electrons diffract as on a regular grid and constructively interfere in diffraction spots at a certain distance from the sample. The pattern of diffraction spots is then an image of the crystalline surface structure in reciprocal space. Thus, the inverse of unit cell lengths can be measured in the LEED pattern relative to the inverse of a known unit cell length. In this way the unit cell of an adsorbed super-structure relative to the unit cell of the substrate can be determined more accurately than using microscopy. An example is shown in Figure 2.7(b) where a unit cell seven times as large as the substrate unit cell is observed.

2.5.2   Components

The general components for LEED, as shown in Figure 2.7(a), are an electron gun, four hemispherical electrostatic grids with the sample at their center, and a hemispherical fluorescent screen outside of the grids. In detail, the cathode filament in the electron gun produces free electrons. These are collimated by a Wehnelt cylinder and accelerated to the desired energy by an electrostatic lens. This is achieved by holding the cathode filament on a negative potential with respect to the lens, the sample, and the first grid, which are grounded. When impinging on the sample, not all electrons are scattered elastically as described above but can be scattered inelastically as well. The second and third grid are held on a negative potential in order to prevent the inelastically

scattered electrons from reaching the screen and causing a background. The fourth grid is again grounded in order to shield the other grids from the high voltage on the fluorescent screen. This is needed to accelerate the electrons into the screen with enough energy to cause fluorescence at the position of impingement. The LEED pattern on the fluorescent screen can be observed through a viewport of the UHV chamber using any conventional camera.